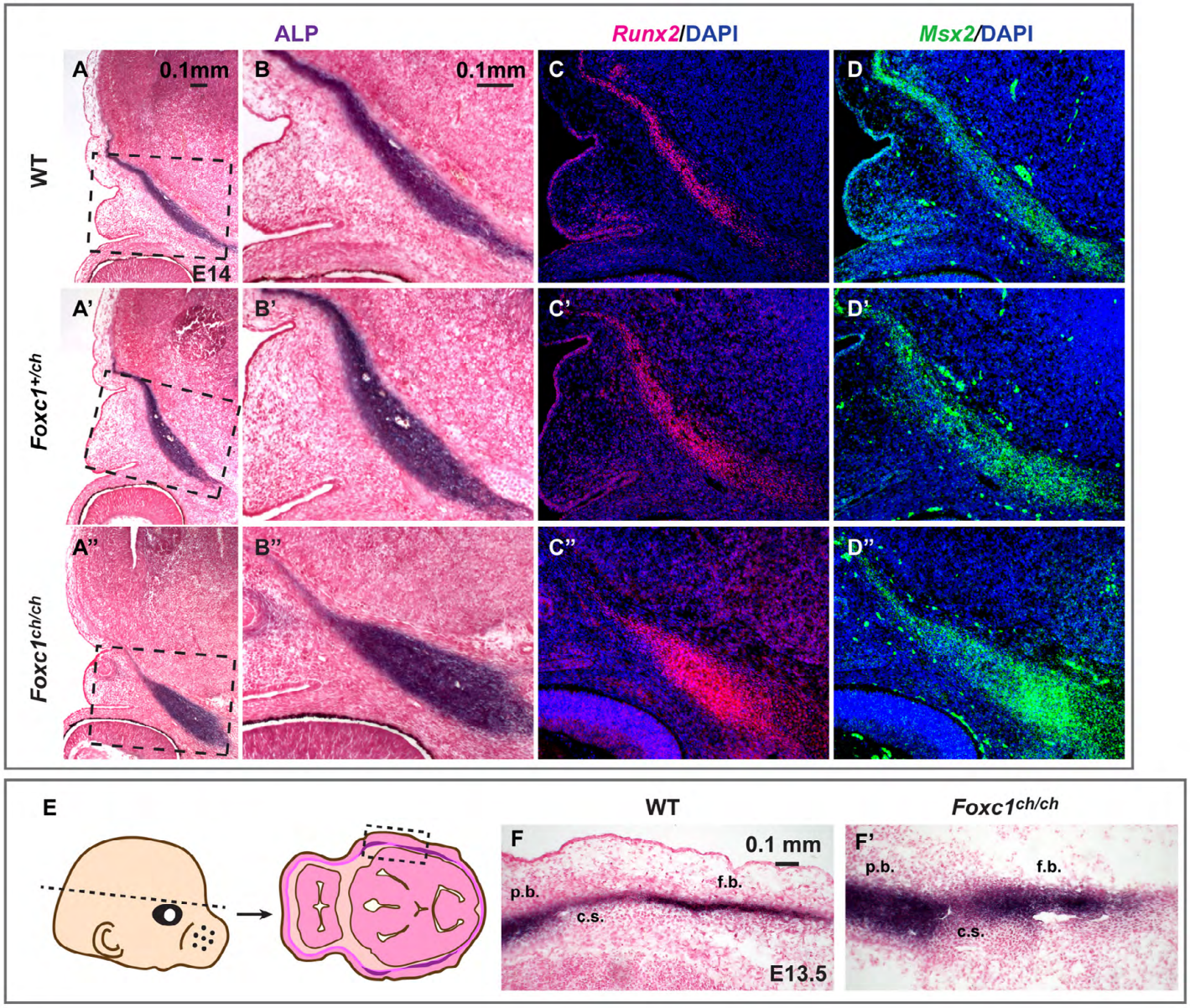

Fig. S1. *Foxc1* dose-dependant expansion of the osteogenic domain in frontal and parietal bone rudiments. (**A-D″**) We detected ALP activity, *Runx2* and *Msx2* mRNA in adjacent sections from E14 wild-type, heterozygous and homozygous *Foxc1* mutant embryos. There is *Foxc1* dose-dependant expansion in ALP, and *Runx2* and *Msx2* expression domains at the cranial base. *Runx2*, also a marker for osteoblast differentiation, is expressed in a similar manner to ALP in both wild-type and *Foxc1* mutant embryos (C′,C″). (**E**,**F′**) Transverse sections through the coronal suture immediately above the eyes (shown in E) from E13.5 wild-type and *Foxc1* mutant embryos were stained for ALP. There is an increase in the thickness of the osteogenic tissue layers in both frontal and parietal rudiments in the *Foxc1* mutant and the the coronal suture narrows. f.b., frontal bone rudiment; p.b., parietal bone rudiment; c.s., coronal suture.

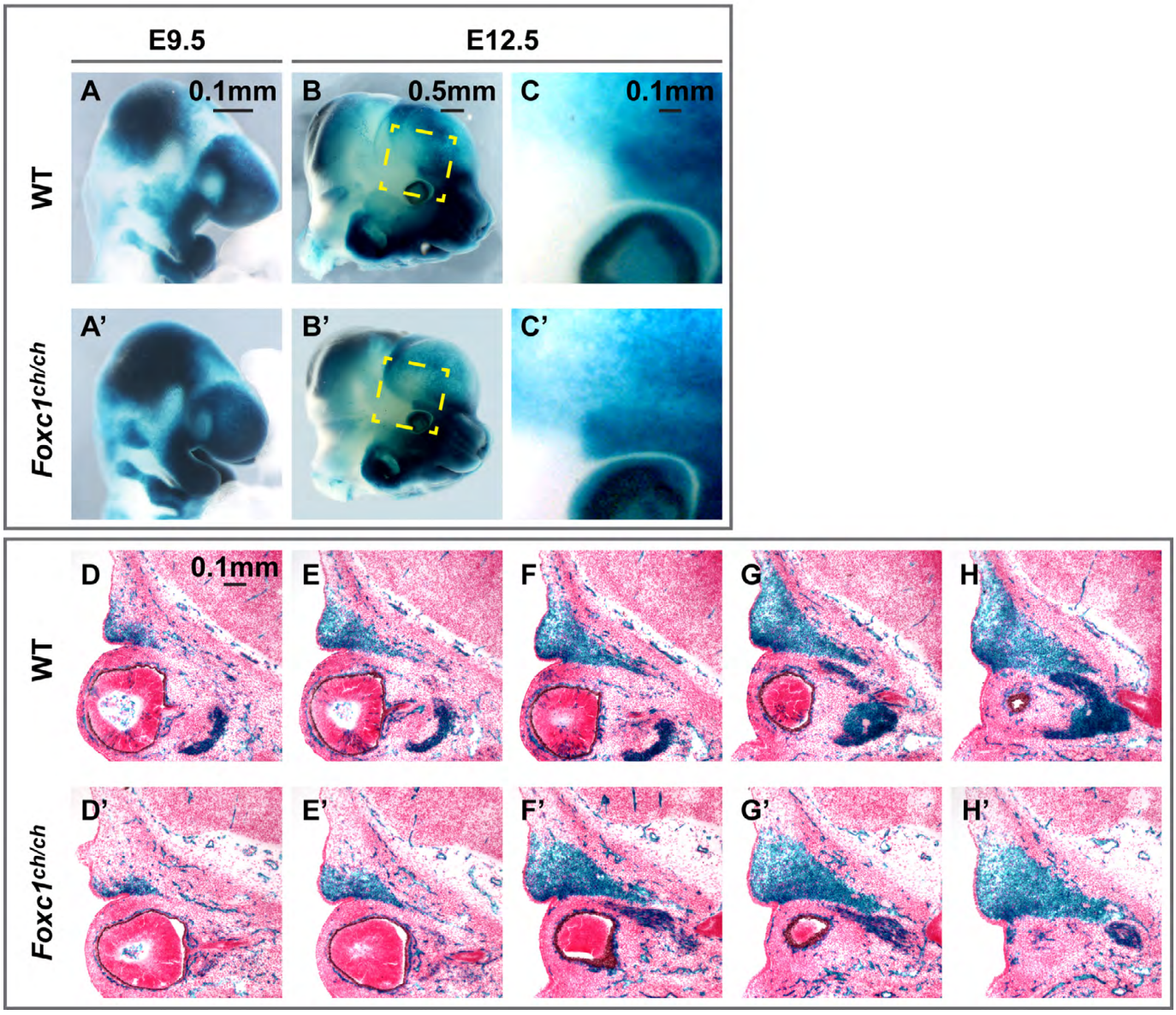

Fig. S2. Distribution of cranial neural crest and head mesoderm in *Foxc1* mutant embryos. (**A-H′**) Neural crest-derived cells were labeled with *Wnt1-Cre; R26R-lacZ* (A-C′) and mesoderm-derived cells with *Mesp1-Cre; R26R-lacZ* (D-H′). We carried out whole-mount staining for β-galactosidase of wild-type and *Foxc1* mutant embryos at E9.5 and E12.5. At both stages, the gross distribution of neural crest cells was almost indistinguishable in the mutant versus wild-type embryos (A′,B′ versus A,B), the only apparent difference being a slight posterior shift of the neural crest population in the supraorbital ridge in *Foxc1* mutants (C,C′). (D-H′) Sections from E12.5 *Mesp1-Cre; R26R-lacZ* embryos of wild-type and *Foxc1* mutant background were stained for *lacZ*, revealing a distribution of neural crest and mesoderm consistent with the whole mounts shown in A-C and A′-C′.

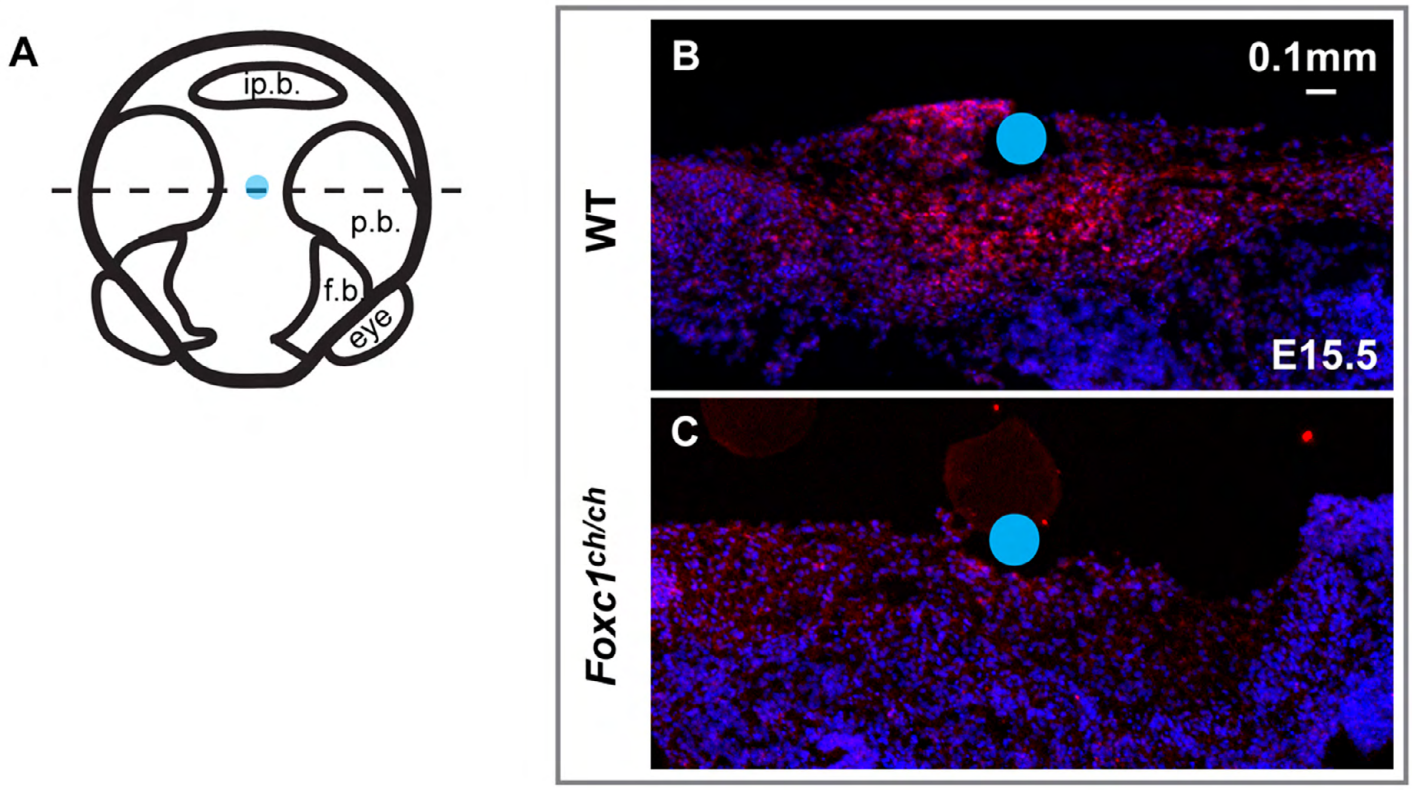

Fig. S3. Reduced BMP-responsiveness of *Msx2* in *Foxc1*$^{ch/ch}$ embryonic head at E15.5. (**A-C**) We excised the dorsal regions of E15.5 wild-type and *Foxc1*$^{ch/ch}$ heads and placed them in organ culture as described previously (Rice et al., 2003). BMP2-soaked beads were implanted in the dorsal midline as indicated in A and the explants were cultured for 48 hours. They were then fixed, sectioned and subjected to in situ hybridization for *Msx2*. Note the substantially greater *Msx2* signal (red color) in the wild type (B) compared with the *Foxc1*$^{ch/ch}$ explant (C).

Table S1. Sequences of siRNA and primers for RT-PCR and ChIP analysis

siRNA	**sense**	**antisense**
GFP	5'-GAC GUA AAC GGC CAC AAG UTT-3'	5'-ACU UGU GGC CGU UUA CGU CTT-3'
RT-PCR	**forward**	**reverse**
Foxc1	5'-CGG CAC TCT TAG AGC CAA AT-3'	5'-TTT GAG CTG ATG CTG GTG AG-3'
Msx2	5'-AAT TCC GAA GAC GGA GCA C-3'	5'-CTT CCG GTT GGT CTT GTG TT-3'
ALP	5'-TGA CCT TCT CTC CTC CAT CC-3'	5'-CTT CCT GGG AGT CCTC ATC CT-3'
Runx2	5'-CCT GAA CTC TGC ACC AAG TC-3'	5'-GAG GTG GCA GTG TCA TCA TC-3'
Osteocalcin	5'- AGA CAA GTC CCA CAC AGC A-3'	5'- CTG CTT GGA CAT GAA GGC -3'
Gapdh	5'-ACC ACA GTC CAT GCC ATC AC-3'	5'-TCC ACC ACC CTG TTG CTG TA-3'
ChIP	**forward**	**reverse**
endogenous *Msx2* enhancer	5'-TCT GCC CAG TTG GAG GTT TGA-3'	5'-GCC GCG TTA ATT GCT CTC G-3'
β-Actin promoter	5'-AGC TTC TTT GCA GCT CCT TCG TTG-3'	5'-ATC TTC TCC ATG TCG TCC CAG TTG-3'
hsp68 mini promoter	5'-GAG CTC CAG GAA CAT CCA AA-3'	5'-GAT CCT CTC CAA TCG CGT TA-3'